

# RF, Pulsed-IV, Device Measurement System in VXI

Jonathan Scott<sup>†</sup>, Anthony Parker<sup>◊</sup>, and Mohamed Sayed<sup>‡</sup>

<sup>†</sup>Department of Electrical Engineering, University of Sydney, 2006, Australia

Facsimile:+61(2)351-3847, Phone:+61(2)351-3294, e-mail:jbs@ee.su.oz.au

<sup>◊</sup>Department of Electronics, Macquarie University, Australia

<sup>‡</sup>Hewlett-Packard Company, SRSD, Santa Rosa, CA 95403, USA

This paper describes a VXI-based, Pulsed-IV, device measurement system. Intended for characterising RF and microwave (high-speed) devices, it combines digital stimulus sources, amplifiers and digitisers with an embedded computer to permit model extraction. It can acquire arbitrary stimulus-response data to high precision very quickly. This versatile platform sees application in research because of its flexibility, but also in production situations owing to its speed. Application examples are given.

## 1 Introduction

For some years now, it has been plain that RF devices made of III-V semiconductor are so field and temperature sensitive, that conventional (“dc”) curve tracers (semiconductor parameter analysers or SPAs) provide insufficient information to characterise even simple device properties such as  $g_m$ . This problem has been investigated previously by combining conventional instruments such as oscilloscopes and pulse generators.[1] The present instrument has evolved in response to the need for a dedicated instrument to measure a series (grid) of characteristic data of a device under fast, pulsed conditions

1. using pulses of less than  $1\mu s$ , to over 10ms,
2. with stimulus voltages of  $\pm 20$ Volts,
3. with peak currents of at least  $\pm 1$ Amp,
4. spanning thousands of measurement points,
5. with high potential precision and linearity (12 bits),
6. with the flexibility to achieve unusual, complex stimulus-response regimes,
7. remaining integrable with S-parameter measurements,
8. expanding speed and power as future modules become available,

9. with duty cycle reaching at least as low as 0.1%, and

10. very quickly.

This system meets these requirements, and can be accommodated within a single VXI rack, in addition to probes. The ability to obtain a very wide range of stimulus signals and timing is not available by any other means. (For instance, virtually any test waveform may be programmed, with 6.25ps event resolution.) The system’s arbitrary nature leads to the acronym APSPA, for arbitrary pulsed semiconductor parameter analyser, after the old HP4145A SPA upon which the idea was originally based.

## 2 System Hardware

Figure 1 shows the prototype system’s various instruments in a VXI rack. The connectivity of the instruments is depicted in figure 2. An example timing diagram is shown in figure 3. Integration of an 85108 is straightforward: synchronising signals are already provided by the APSPA timing module, and bias tees can be connected as shown in figure 4. Figure 4 shows a preferred method of connecting a FET device (no gate current measurement). Integration of HP85120A pulsers is also straightforward: Figure 5 shows the required changes.

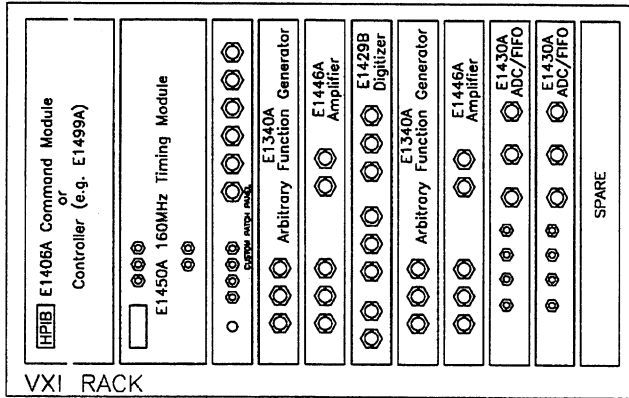


Figure 1: The VXI rack recommended layout.

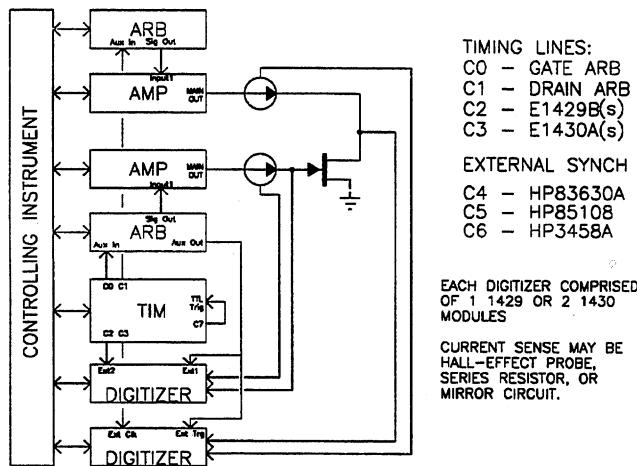


Figure 2: The instrument connectivity diagram.

Current sensing may take various forms, such as a Hall-effect current probe. Our experience is that the Tektronix AM503A system is very linear to 50MHz.

### 3 Application Example

Figures 6 and 7 show the characteristics of an MGF-1400 MESFET determined conventionally and using the PIV system. Consider this device operating as a class-A amplifier. The expected small-signal gain can be estimated using the formula

$$A_v = g_m \times (R_L \parallel r_o) \quad (1)$$

where  $g_m$  and  $r_o$  are parameters estimated from the characteristic of the device. Using estimates of these parameters made from conventional HP4145A-derived data about the point

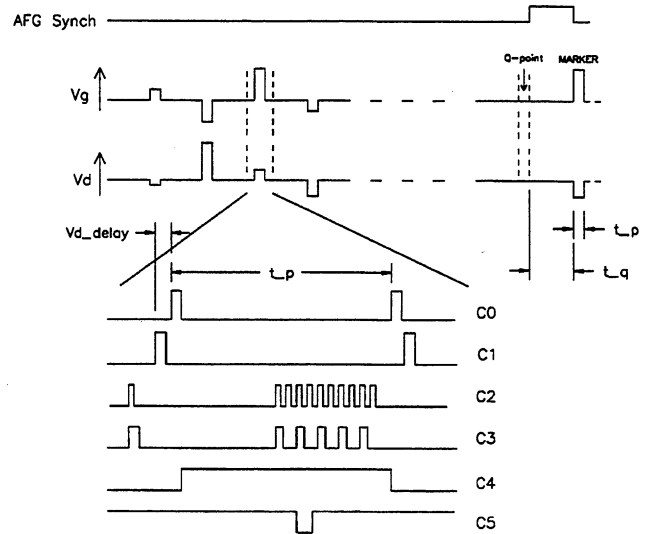


Figure 3: A typical example timing diagram for the APSPA system. Details alter automatically with user-specified durations and preset delays.

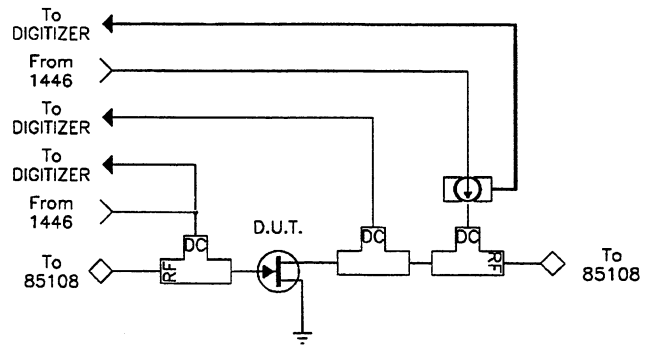


Figure 4: Connection of bias tees for integrated S-parameter measurements.

$V_{gs} = 0V$  and  $V_{ds} = 2V$ , a value of  $\approx 22$  is obtained for  $R_L = 500\Omega$ . Using the PIV equivalent data from figure 7, a value of  $A_v \approx 10$  is obtained. Subsequent measurement gives a value of  $\approx 11$ .

### 4 A New Dimension in RF-Device Characterisation

The above application example demonstrates the need for designers to employ PIV systems, in order to provide useful estimates of conventional parameters. The next highlights the ability to give insight into previously invisible aspects of device behaviour.

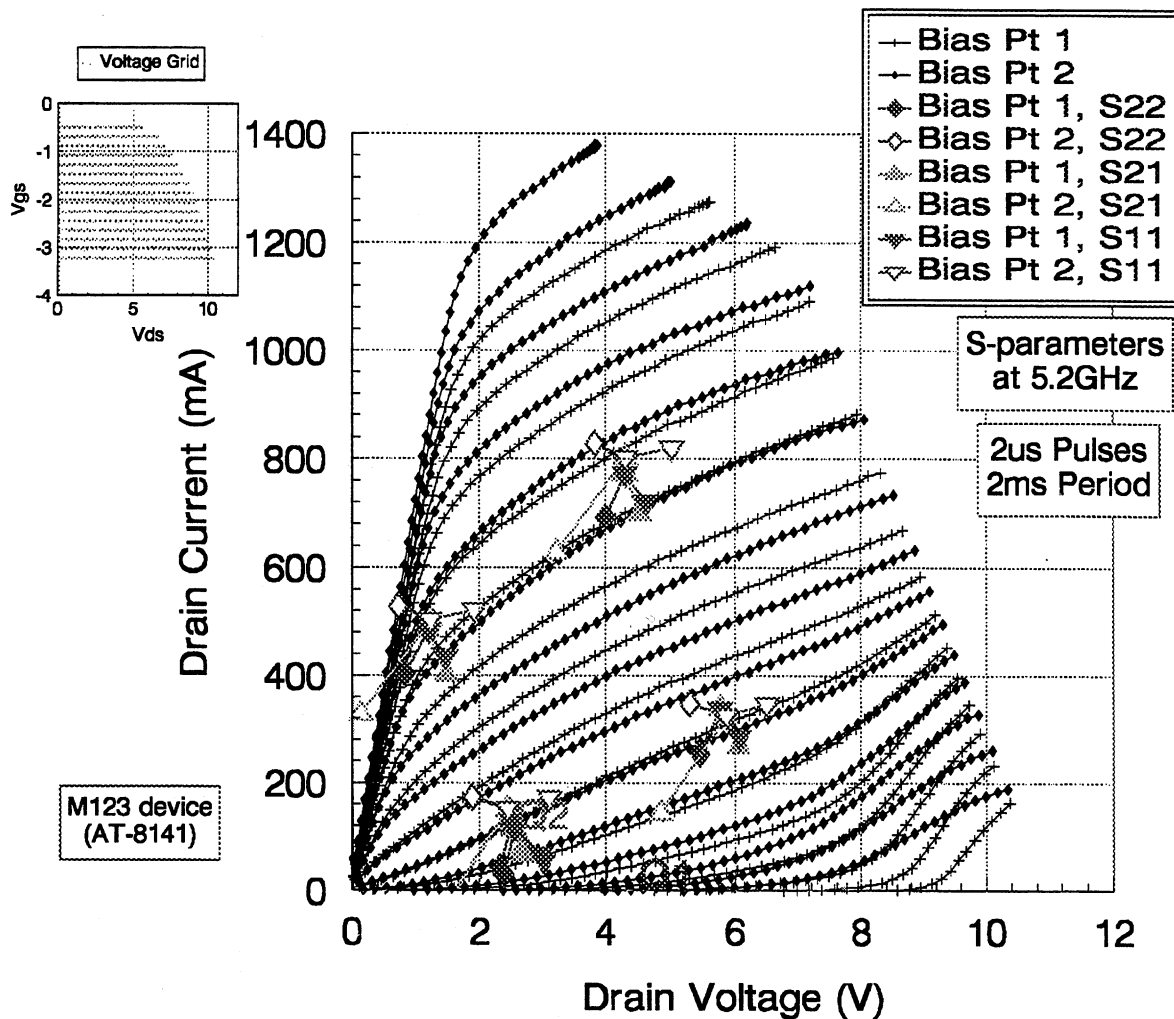


Figure 8: Example of S-parameter and PIV data collected on a common low-noise GaAs device. The overlaid vectors show the change in S-parameters with a change in bias point, *measured at identical instantaneous points*. Each S-vector shows the magnitude and phase of the designated s-parameter.

#### 4.1 Transient Behaviour Characterisation

Figure 8 uses the capacity of the system to measure not only PIV data, but synchronised with S-parameters, at any point in the I-V plane, *and* for any required quiescent point. (This graph requires some study in order to resolve the large amount of data presented.) The message is that the *instantaneous* S-parameters of a device, representing its behaviour during a signal excursion through a point in the IV plane, are a function of the bias point about which the excursions are centred. In performance terms, this means not only that the transient, large-signal behaviour can be

expected to vary with bias point, but that the behaviour will be predictable, based upon characterisation using a PIV system such as this.

## 5 Acknowledgement

This work has been supported by the Department of Industry, Science and Technology under a Bilateral Science and Technology Grant. The authors are grateful to DIST and Hewlett-Packard's Custom Systems Division for their assistance.

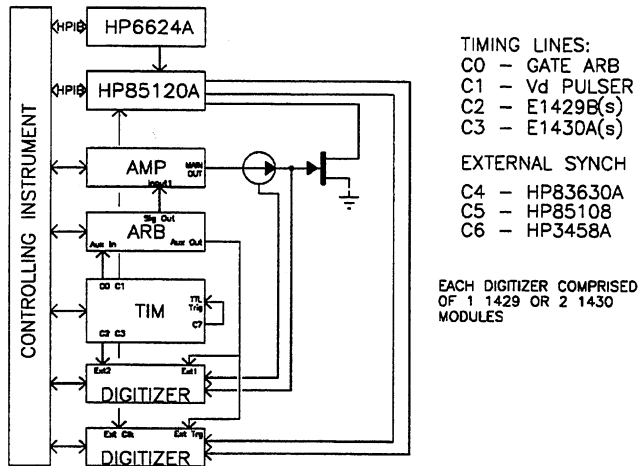


Figure 5: The instrument connectivity diagram when using HP85120.

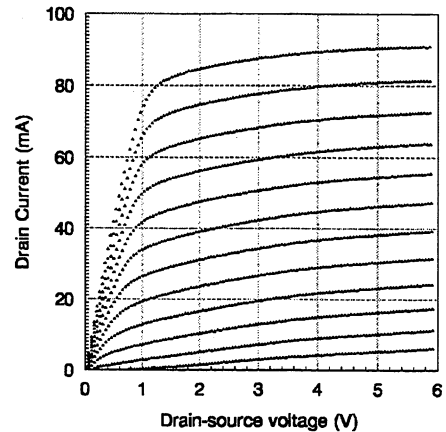


Figure 7: The  $I_d$  vs.  $V_{ds}$  characteristic of a MESFET measured using short ( $2\mu s$ ) pulses with 1% duty cycle about a bias point of  $V_{gs} = 0V$  and  $V_{ds} = 2V$ .

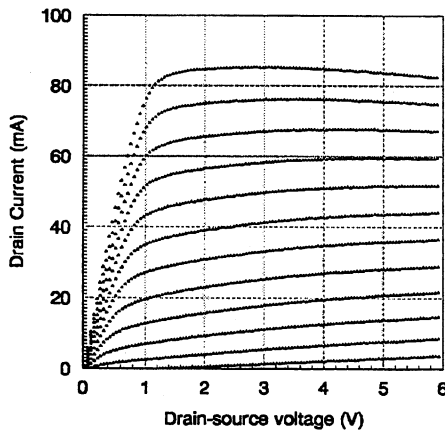


Figure 6: The  $I_d$  vs.  $V_{ds}$  characteristic of a MESFET measured at conventional (millisecond) speeds.

## References

- [1] Anthony Parker and Jonathan Scott, "New Method for Comprehensive Characterisation of MES/MOD/MOS FETs", *Proceedings of the IEEE International Symposium on Circuits and Systems*, Chicago, 3-6 May, 1993, pp1093-1096.
- [2] J B Scott, D R Webster, A E Parker, D G Haigh, James P M Proctor and Oliver J Ridler, "Improved Characterisation of FET Non-linear Behaviour", *Asia-*

*Pacific Microwave Conference*, December 6-9, Tokyo, Japan, pp635-638.

- [3] W. Struble, S. L. G. Chu, M. J. Schindler, Y. Tajima and J. Huang, "Modelling Intermodulation Distortion in GaAs MESFETs using Pulsed I-V Characteristics", *Technical Digest of the IEEE GaAs IC Symposium*, Monterey, California, October 20-23, 1991, pp179-182.
- [4] Jonathan Scott and Anthony Parker, "Trends in Device Characterisation: A Pulsed Semiconductor Parameter Analyser System for III-V FETs", *Journal of Electrical and Electronics Engineering, Australia*, vol. 14, no. 3, September 1994, pp. 196-205.